International Journal of Computational Methods
Vol. 14, No. 1 (2017) 1750002 (11 pages)

DOI: 10.1142/S0219876217500025

Two-Dimensional Simulations of Turbulent Flow Past a Row of Cylinders using Lattice Boltzmann Method

Yi-Kun Wei

Faculty of Mechanical Engineering and Automation
Zhejiang Sci-Tech University
Hangzhou 310018, P. R. China
ykun_wei@sina.com

Xu-Qu Hu*

State Key Laboratory of Advanced Design
and Manufacturing for Vehicle Body
College of Mechanical and Vehicle Engineering
Hunan University, Changsha 410082, P. R. China
huxuqu@gmail.com

Received 1 December 2015
Accepted 9 March 2016
Published 31 May 2016

Two-dimensional simulations of channel flow past an array of cylinders are carried out at high Reynolds numbers. Considering the thickness fluctuating effect on the equation of motion, a modified lattice Boltzmann method (LBM) is proposed. Special attention is paid to investigate the thickness fluctuations and vortex shedding mechanisms between 11 cylinders. Results for the velocity and vorticity differences are provided, as well as for the energy density and enstrophy spectra. The numerical results coincide very well with some published experimental data that was obtained by turbulent soap films. The spectra extracted from the velocity and vorticity fields are displayed from simulations, along with the thickness fluctuation spectrum H(k). Our results show that the statistics of thickness fluctuations resemble closely those of a passive scalar in turbulent flows.

Keywords: Lattice Boltzmann method; thickness fluctuating; energy spectra.

1. Introduction

The unsteady flow of Newtonian fluids around multiple bluff bodies is an important problem for both fundamental research and applications [Kellay *et al.* (1998); Abdel Kareem *et al.* (2014)]. A typical example is the two-dimensional (2D) turbulent flow past a row of cylinders, which is frequently encountered in many practical situations such as turning vanes in duct elbows, multi-slotted airfoils and flow

*Corresponding author.

around closely spaced power poles [Kumar *et al.* (2008)]. During the past decades, an increasing number of researchers have paid their attention on this topic, and many progresses have been done using experimental or/and numerical techniques, e.g., see Rahmati [2009], Chatterjee *et al.* [2010] and Chang and Constantinescu [2015].

The lattice Boltzmann method (LBM), which considers collision models and solves discrete Boltzmann equation to simulate the flow of a Newtonian fluid, is a relatively new approach in Computational Fluid Dynamics [Qian (1993); Chen and Doolen (1998)]. Owing to its particulate nature and local dynamics, the LBM has distinct advantages in dealing with complex boundaries and in performing the parallel computations with high efficiency, both of which meet the demand of an appropriate numerical model for the flow past a row of cylinders. Therefore, it has been widely applied in numerical simulations on this topic and rich phenomena were discovered. Agrawal *et al.* [2006] investigated the flow through a pair of square cylinders using a 2D LBM. Their results have proven the existence of both synchronized and flip-flop regimes with square cylinders. Kumar *et al.* [2008] studied the flow at a low Reynolds number (Re=80) around a row of square cylinders using LBM. Three flow regimes (synchronized, quasi-periodic, and chaotic) were revealed by vorticity field and drag coefficient signal, which were mainly caused by the interaction between primary (vortex shedding) and secondary (cylinder interaction) frequencies. Chatterjee *et al.* [2010] have numerically studied the flow around a row of square cylinders at a higher Reynolds number (Re=150), with their specific attention on the effect of the spacing between the cylinders on the wake structure and vortex shedding mechanism. Several LBM numerical simulations have also been carried out for cylinders [Li *et al.* (2004); Nemati *et al.* (2010)]. However, most of these studies are under the assumption of a relatively low Reynolds number.

For relatively high Reynolds numbers, the thickness fluctuation is an unavoidable phenomenon in turbulent flows. Over the past two decades, several experimental studies were carried out to measure the thickness fluctuation. Kellay *et al.* [1998] have utilized two optical-fiber velocimeters to measure the vorticity fluctuations in rapidly flowing turbulent soap films driven by gravity. Vorobieff *et al.* [1999] have measured the simultaneous velocity and thickness fields in the flow past cylinders. Belmonte *et al.* [1999] have investigated the quasi-2D decaying turbulence in a flowing soap film by measuring the moments of the probability density function for the longitudinal velocity differences. Greffier *et al.* [2002] measured the rapid fluctuations of the film thickness in turbulence, and they found that the scalar spectra can be well described by Kolmogorov-like scaling. Many experimental results have proven a strong correlation between thickness fluctuations and vorticity fields, it is thus important to take the effect of thickness fluctuating into account in numerical simulations. However, the related literatures are not many by now. All the numerical simulations have been done using a lattice Boltzmann scheme. LBM are well known and widely applied to a variety of single, multiphase and thermal fluids hydrodynamic problems [Qian *et al.* (1992); Shan (1997); Chen and Doolen (1998); He *et al.* (1998); Succi (2001); Aidun and Clausen (2010); Abdel Kareem *et al.* (2014)].

In the present study, we focus on the turbulent flow around a row of side-by-side circular cylinders. Firstly, a modified LBM is proposed to consider the thickness fluctuating effect on the motion equations. After the problem definition and numerical verification, the flow at a relatively high Reynolds number (Re=500) is numerically studied using this modified LBM. The underlying mechanism such as turbulent energy, entropy spectra, thickness fluctuation, and vorticity contours of the steady state are all carefully examined and discussed. Finally, some concluding remarks are presented.

2. Vorticity-Thickness Coupling

In soap film experiments, vorticity and thickness fluctuations are normally produced by inserting objects into flow domain, for example, cylinders were used in Vorobieff *et al.* [1999]. At a relatively large flow rate, the fluid that is drawn off from the meniscus surrounding the cylinder wraps around the vortex core, and the thickness fluctuations are shed from the solid surface coincidentally with the vortex shedding. The vorticity and thickness in films are therefore initially correlated. A strong correlation between thickness fluctuations and the vorticity fields were proposed in some pioneering experimental studies [Vorobieff *et al.* (1999); Greffier *et al.* (2002)]. For example, Vorobieff *et al.* [1999] have assumed that the thickness is advected as a passive scalar, and successfully explained the persistence of initial correlation in the downstream flow. Following these pioneering work, we have derived the macroscopic equation of thickness fluctuations in the following section.

Under the limit of passive scalar, both vorticity and thickness obey the convective diffusive equations [Vorobieff *et al.* (1999)]:

$$\frac{D\omega}{Dt} = \frac{\partial \omega}{\partial t} + u \cdot \nabla \omega = \nu \nabla^2 \omega, \tag{1}$$

$$\frac{Dh}{Dt} = \frac{\partial h}{\partial t} + u \cdot \nabla h = \kappa \nabla^2 h, \tag{2}$$

where ω is the fluid vorticity and h denotes the thickness. The two equations only differ from each other by their respective diffusion constants, they are ν and κ, respectively. Both diffusion constants are very small. In unchanged flow, the thickness and velocity fluctuations are associated together, and the correlation between vorticity and thickness fields persists in downstream. Therefore, the correlation cannot grow beyond its initial value behind the comb under the assumption that the fluid is incompressible. Considering the effect of thickness fluctuation on the equation of motion, the Navier–Stokes equation can be expressed as following,

$$\frac{\partial u}{\partial t} + u \cdot \nabla u = -\frac{C^2}{h_0} \nabla h - \frac{1}{\rho} \nabla P + \nu \nabla^2 u, \tag{3}$$

where h_0 is the initial thickness, $C = \sqrt{E/\rho h_0}$ denotes the velocity of elastic waves on the soap film, E and ρ are the elastic modulus and the density of water, respectively. The continuous equation is expressed as following,

$$\frac{\partial \rho}{\partial t} + \nabla \cdot (\rho u) = 0. \tag{4}$$

3. Modified LBM

In order to satisfy Eqs. (3) and (4), we propose a modified equilibrium distribution functions as below,

$$f_i^{\mathrm{eq}} = \begin{cases} w_i \rho \left(1.0 + \dfrac{c_{i\alpha} u_\alpha}{c_s^2} + \dfrac{c_{i\alpha} c_{i\beta}}{2c_s^4} - \dfrac{u^2}{2c_s^2}\right) + w_i \dfrac{E}{h_0} \dfrac{h}{c_s^2} \\ w_0 \rho \left(1.0 + \dfrac{c_{i\alpha} u_\alpha}{c_s^2} + \dfrac{c_{i\alpha} c_{i\beta}}{2c_s^4} - \dfrac{u^2}{2c_s^2}\right) - \left(\sum_i w_i\right) \dfrac{E}{h_0} \dfrac{h}{c_s^2} \end{cases} \quad (i = 1 \ldots), \tag{5}$$

where the subscripts α and β denote the Cartesian components, i denotes the number of lattice velocities, and w_i is the weight coefficient. A particle velocity belongs to a discrete and limited set c_i, while c_s denotes the sound speed. The applied numerical algorithm is based on discrete kinetic models. The starting point is a standard Lattice Boltzmann equations described by the following expressions,

$$f_i(x + c_i \Delta t, t + \Delta t) = f_i(x, t) + \frac{1}{\tau_1}(f_i^{\mathrm{eq}} - f_i(x, t)), \tag{6}$$

where $\tau_1$denotes the relaxation time. As the thickness fluctuation equation (2) has a very similar form as the diffusion equation, we can use the diffuse equation to simulate the thickness fluctuation in the following section. The equilibrium distribution function of diffuse equation can be expressed as following,

$$g_i^{\mathrm{eq}} = w_i h \left[1 + \frac{c_{i\alpha} u_\alpha}{c_s^2}\right]. \tag{7}$$

In order to recover the thickness fluctuation equation, we need to add an additional term in the LBGK equations, which has a form as

$$g_i(x + c_i \Delta t, t + \Delta t) = g_i(x, t) + \frac{1}{\tau_2}(g_i^{\mathrm{eq}} - g_i(x, t)) - w_i v_{i\alpha} \frac{\partial h}{\partial x_\alpha}, \tag{8}$$

where $g_i(x, t)$ is the distribution function of thickness fluctuation, $\tau_2$is the relaxation time, $v_{i\alpha}$ represents extra viscous terms, and w_i denotes the weight coefficient. We can derive Eqs. (2)–(4) from Eqs. (5)–(9) using the Chapman–Enskog and Taylor expansion methods. The viscosity coefficient and the diffusion coefficients are expressed as follows,

$$\nu = c_s^2 \left(\tau_1 - \frac{1}{2}\right) \Delta t, \quad \kappa = c_s^2 \left(\tau_2 - \frac{1}{2}\right) \Delta t, \quad P = \rho c_s^2. \tag{9}$$

Just like the method to construct a conventional LBM, we can also derive the conservation criteria between the macroscopic physical quantities and microscopic particle populations,

$$\begin{bmatrix} \rho \\ \rho u \\ PI + (E/h_0^2)h + \rho uu \end{bmatrix} = \begin{bmatrix} \sum\limits_i f_i^{\text{eq}} \\ \sum\limits_i c_i f_i^{\text{eq}} \\ \sum\limits_i c_i c_i f_i^{\text{eq}} \end{bmatrix}, \tag{10}$$

where the correlation between the macroscopic physical quantities and microscopic particle populations can be expressed as following,

$$\rho = \sum_{i=0}^{8} f_i, \quad \rho u = \sum_{i=0}^{8} c_i f_i, \quad h = \sum_i g_i. \tag{11}$$

Considering the conservation criteria between the macroscopic physical quantities and microscopic particle populations in Eq. (10), we use a Chapman–Enskog expansion to deduce the equations for density, momentum, and temperature from Eqs. (6)–(8). At the streaming step, the left-hand side of Eq. (10) can be used to reproduce the inertial terms in the thickness equation and the Navies–Stokes equations. For the effect of thickness fluctuation, we can determine the thickness fluctuation h from the modified equilibrium distribution function and the mesoscopic equation, as mentioned in Eq. (5). The determined thickness fluctuation h can be used to recover the relation of ∇h in the momentum equation of Eq. (3), and therefore, the effect of thickness fluctuating is taken into account in our modified LBM model.

For the part of energy, the selection of the initial conditions is important to the simulation. A customary choice is to start with some power law, for example, $E(k) \sim Ck^{-p}$, where the phase is made randomly. In principle, this can be obtained by selecting appropriate velocity field $\hat{u}_i(\mathbf{k})$ in wave number space.

Owing to the homogeneous character of the flow, this velocity field needs to satisfy the limit of energy spectrum and continuous function,

$$E(k) = \frac{1}{2} \int \hat{u}_i(\mathbf{k}) \hat{u}_i^*(\mathbf{k}) dk, \tag{12}$$

where $\hat{u}_i^*(\mathbf{k})$ is the complex conjugate of $\hat{u}_i(\mathbf{k})$, and $S(\mathbf{k})$ denotes a circle with radius equal to $k = |\mathbf{k}|$. More details about the methods to get $\hat{u}_i(\mathbf{k})$ can be found in Kellay *et al.* [1998] and Agrawal *et al.* [2006].

4. Results and Discussions

In the present study, we have considered that 11 fixed cylinders with diameter d(characteristic length scale) are exposed to a constant flow with uniform velocity U_0. Distance between cylinders is equal to the diameter of a cylinder. The width of the computational domain (L_x) is taken to be $30d$, while the length of the computational domain (L_y) is taken to be $300d$. The initial thickness h_0 is $0.001d$. According to the conversion relationship between macroscopic and LBM, the viscosity coefficient ν takes the value of $1.01{*}10^{-3}$, and the diffusion coefficient κ is 0.55

in our simulations. We have implemented 2,000×200 lattices to discretize the computational domain. We have also checked the influence of mesh size using a mesh twice as small as that described above and have not found significant influence on the final results. The velocity boundary condition has been applied on the lateral sides of the computational domain for extending the results to an infinite number of cylinders. The no-slip condition on the fluid–solid interfaces is executed in all simulations. A uniform velocity with negligible compressibility effect (U_0/c=0.0799) is prescribed at the inlet. A convective boundary condition has been used at the outlet, which allows an unconstrained movement of the fluid away from the computational domain. A relatively high *Reynolds* number Re= 500 is implemented in our simulations. A new equilibrium distribution function is carried out to simulate the Navies–Stokes equation, and the D2Q5 model is used to simulate the thickness fluctuation equation.

Figure 1 shows the vorticity contours at the steady state. It demonstrates the past flow in distance of $20d$ from cylinder to downstream. We can find that the vortices in the downstream near cylinders are not quite clear, and some of the vortices become narrower or wider than the normal vortices. It is mainly caused by the fact that the flow interference between successive cylinders is quite strong at this small separation ratio, and consequently, oscillating regions are found to exist together. Furthermore, it can be seen that the flow characteristics is mainly determined by the jet flow in the gaps between consecutive cylinders. The jets merge behind the cylinders. The shed vortices are strongly interacted by the jets. Because of the interaction of multiple frequencies, the natural frequency of vortex shedding and the jet-induced frequency "combined frequencies" both arise. The flow behavior

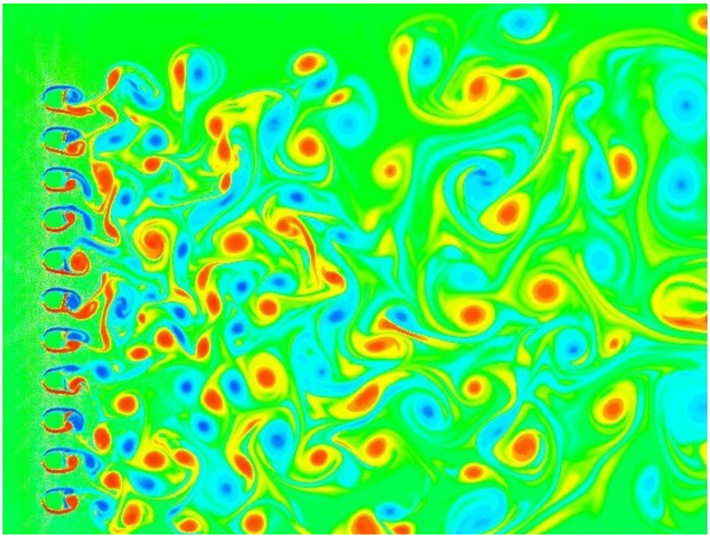

Fig. 1. Vorticity contour at the steady state.

Fig. 2. Vorticity streamlines from cylinders in the synchronized regime.

is in good agreement with some experimental results, for example, in Kellay *et al.* [1998] and Agrawal *et al.* [2006].

To show the frequency of vortex shedding, the vorticity streamlines are also displayed from $15d$ to $45d$ in Fig. 2. The shed vortices are interacted by the jets. We can find that the flow is dominated by the presence of vortices interacting very strongly with each other. The gradient of strong vorticity has been well captured by the presence of dark regions in the contour. It is of interest to note that the average size of the vortical structures, which are advected downstream from the grid, seems to grow as the distance from the grid increases. It is possible that the scalar field is less sensitive to strain (enstrophy transfer rate) and more sensitive to the energy transfers to large scales, which occur through vortex mergers in simulation of the inverse energy cascade.

We present the density contours, vorticity contours, and thickness fluctuation of instantaneous steady flow in Fig. 3. These results are indicated as a surprising behavior of the scalar field. In Fig. 3(a), we can find that the vortexes appear behind the cylinders and transfer backward. It is clear in Fig. 3(b) that the small vortexes at the near downstream can merge to form big vortexes. Such thickness inhomogeneity can be visualized by simply viewing the reflection from the film of a monochromatic light source plotted in Fig. 3(c). We can find the thickness variation clearly marks the flow, and it provides a natural way to visualize the vortical structures detaching from the obstacles and interact downstream. Our results show that the statistics of thickness fluctuations resemble closely those of a passive scalar.

With sufficiently high injection rates, the flow is turbulent and self-similar as indicated by previous studies [Kellay *et al.* (1998); Agrawal *et al.* (2006)]. The scaling of velocity or vorticity power spectra has been widely used to examine the features of turbulent flow. Figure 4 shows the enstrophy spectra ($e(f) = \langle|\omega(f)|^2\rangle$)

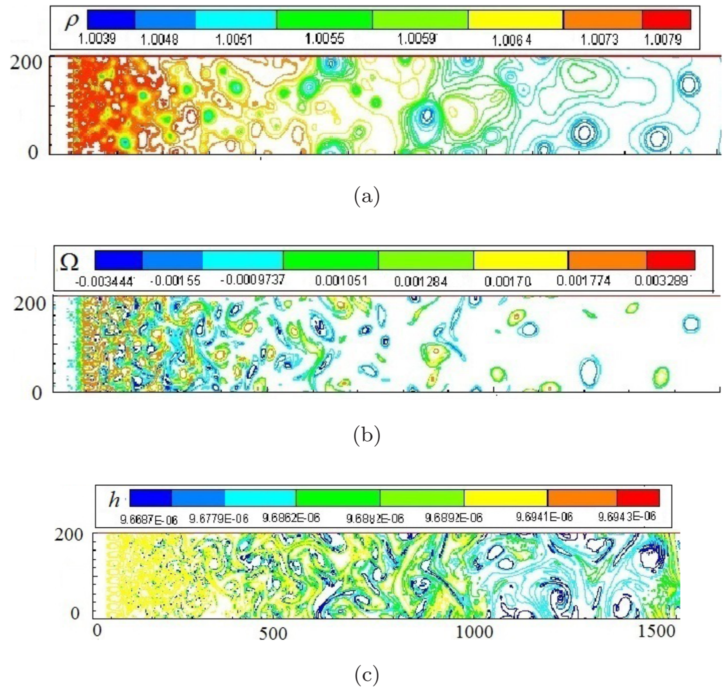

Fig. 3. Instantaneous flow pattern in downstream from the comb. (a) Density contours, (b) vorticity contours and (c) thickness contour.

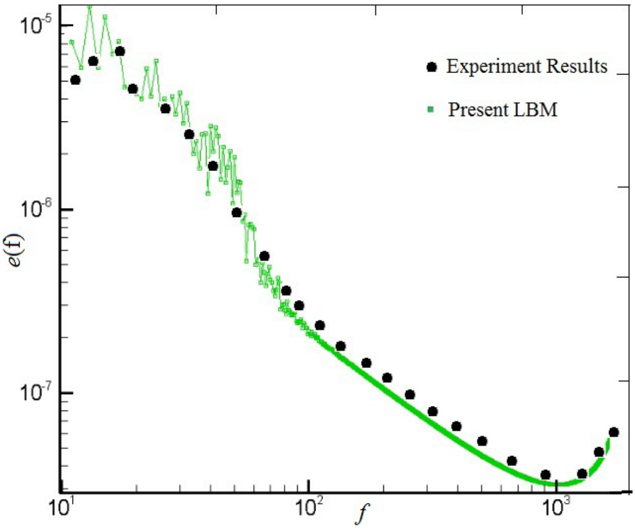

Fig. 4. (Color online) Vorticity power spectrum behind a $5d$ grid.

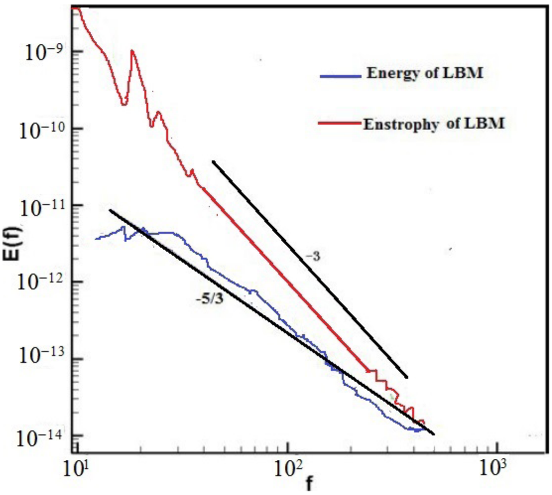

Fig. 5. (Color online) Energy spectra $E(f)$ obtained at the centerline.

measured at the distance of $5d$ behind the cylinders. The green solid squares represent our numerical results, while the black circles are the published experimental results in Kellay *et al.* [1998]. For frequency above about 60 Hz, the spectra decline significantly with the increase of frequency. While frequency exceeds the value of about 10^3, it is full of interest to notice that the enstrophy spectra $e(f)$ increases with the flow rate, and the scaling of numerical simulation becomes more correspondent with that of experiment.

The energy and enstrophy spectra are showed in Fig. 5. The upper green curve is the enstrophy cascade, and the lower blue curve is the energy cascade data. While they are guides to the eye, the straight lines are the expected slopes for the energy and enstrophy cascades. Though the slopes γ in the scaling relation $E(k) \sim k^{-\gamma}$ are only approximately equal to the canonical values $\gamma = 5/3$ (energy) and $\gamma = 3$ (enstrophy). The reason for the departure from 5/3 and 3 is unclear, but it may be closely related to the intermittency studied here. It is further indicated that a k^{-3} scaling is observed in an enstrophy cascade. This deviation from the expected $k^{-5/3}$ scaling is attributed to the presence of large, long-lived coherent structures and finite-size effects in the flow. The main surprise is the existence of Kolmogorov-like scaling for the thickness fluctuations. This entails measuring the wave-frequency spectra of E and e and comparing their scaling exponents to the predicted slopes of k^{-3} for energy and k^{-1} for enstrophy at wave frequency. The spectra extracted from the velocity and vorticity fields are displayed from Fig. 6 along with the thickness fluctuation spectrum H(k). The slopes plotted are nearly k^{-3} on the energy spectrum and k^{-1} on the enstrophy spectrum. As can be seen from Fig. 6, the relation between the thickness fluctuation spectrum (H(f)) and the frequency wave number is presented as $k^{-2.3}$.

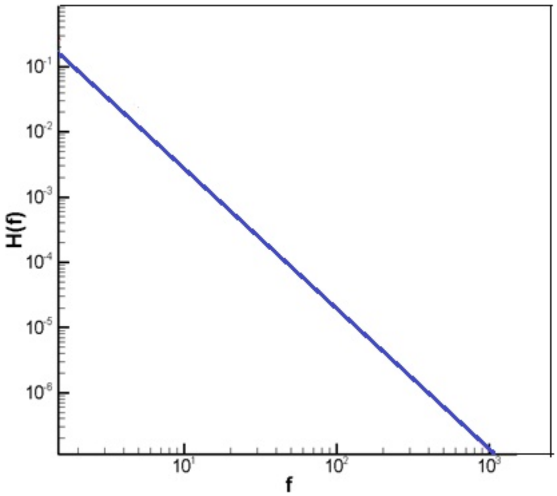

Fig. 6. Thickness spectra $H(f)$ at $5d$ behind the cylinders varying with respect to frequency f.

5. Conclusions

In conclusion, we have presented one of the earliest numerical studies of thickness fluctuations in a 2D turbulent flow past a row of cylinders. In the present study, a modified LBM technique for the simulation of thickness fluctuations in 2D flows is proposed. Our results show that the statistics of thickness fluctuations resemble closely those of a passive scalar. The scaling exponent measured from the vorticity power spectrum of our numerical results coincides very well with previous theoretical predications, and the enstrophy spectra predicated by our numerical model is also in an excellent agreement with experiment results. Furthermore, we have also studied the spectra extracted from the velocity and vorticity fields of numerical results. However, we have to admit that our modified model of LBM can only predicate the effect of thickness fluctuation in a qualitative way, as it is lack of quantitative comparisons with theoretical and experimental data in present study, which can therefore be worthy of further investigations.

Acknowledgments

This work was supported by the National Natural Science Foundation of China (No. 11502237 and 11402084), the Zhejiang Key Discipline of Instrument Science and Technology (No. JL150509-JL150511), the Zhejiang Province Science and Technology Innovation Team project (No. 2013TD18), the Natural Science Foundation of Hunan Province (No. 2015JJ3051) and the Fundamental Research Funds for the Central Universities (Hunan University). We greatly appreciate the reviewer's insightful comments and helpful suggestions.

References

Abdel Kareem, W., Nabil, T., Izawa, S. and Fukunishi, Y. [2014] "Multiresolution and nonlinear diffusion filtering of homogeneous isotropic turbulence," *Int. J. Comput. Methods* **11**(1), 1350054.

Agrawal, A., Djenidi, L. and Antonia, R. A. [2006] "Investigation of flow around a pair of side-by-side square cylinders using the Lattice Boltzmann method," *Comput. Fluids* **35**(10), 1093–1107.

Aidun, C. K. and Clausen, J. R. [2010] "Lattice-Boltzmann method for complex flows," *Annu. Rev. Fluid Mech.* **42**, 439–472.

Belmonte, A., Goldburg, W. I., Kellay, H., Rutgers, M. A., Martin, B. and Wu, X. L. [1999] "Velocity fluctuations in a turbulent soap film: The third moment in two dimensions," *Phys. Fluids* **11**(5), 1196–1200.

Chang, K. and Constantinescu, G. [2015] "Numerical investigation of flow and turbulence structure through and around a circular array of rigid cylinders," *J. Fluid Mech.* **776**, 161–199.

Chatterjee, D., Biswas, G. and Amiroudine, S. [2010] "Numerical simulation of flow past row of square cylinders for various separation ratios," *Comput. Fluids* **39**(1), 49–59.

Chen, S. and Doolen, G. D. [1998] "Lattice Boltzmann method for fluid flows," *Annu. Rev. Fluid Mech.* **30**(1), 329–364.

Greffier, O., Amarouchene, Y. and Kellay, H. [2002]. "Thickness fluctuations in turbulent soap films," *Phys. Rev. Lett.*, **88**(19), 194101.

He, X., Chen, S. and Doolen, G. D. [1998] "A novel thermal model for the Lattice Boltzmann method in incompressible limit," *J. Comput. Phys.* **146**(1), 282–300.

Kellay, H., Wu, X. L. and Goldburg, W. I. [1998] "Vorticity measurements in turbulent soap films," *Phys. Rev. lett.* **80**(2), 277.

Kumar, S. R., Sharma, A. and Agrawal, A. [2008] "Simulation of flow around a row of square cylinders," *J. Fluid Mech.* **606**, 369–397.

Li, Y., Shock, R., Zhang, R. and Chen, H. [2004] "Numerical study of flow past an impulsively started cylinder by the lattice-Boltzmann method," *J. Fluid Mech.* **519**, 273–300.

Nemati, H., Sedighi, K., Farhadi, M., Pirouz, M. M. and Fattahi, E. [2010], "Numerical simulation of fluid flow of two rotating side-by-side circular cylinders by Lattice Boltzmann method," *Int. J. Comput. Fluid Dyn.* **24**(3–4), 83–94.

Qian, Y. H., d'Humières, D. and Lallemand, P. [1992] "Lattice BGK models for Navier-Stokes equation," *EPL (Europhys. Lett.)* **17**(6), 479–484.

Qian, Y. H. [1993] "Simulating thermohydrodynamics with lattice BGK models," *J. Sci. Comput.* **8**(3), 231–242.

Rahmati, M. T. [2009] "Application of a pressure correction method for modeling incompressible flow through turbomachines," *Int. J. Comput. Methods* **6**(3), 399–411.

Shan, X. [1997] "Simulation of Rayleigh-Bénard convection using a Lattice Boltzmann method," *Phys. Rev. E* **55**(3), 2780–2788.

Succi, S. [2001] *The Lattice Boltzmann Equation: for Fluid Dynamics and Beyond* (Oxford University Press, Oxford).

Vorobieff, P., Rivera, M. and Ecke, R. E. [1999] "Soap film flows: Statistics of two-dimensional turbulence," *Phys. Fluids* **11**(8), 2167–2177.